JFE TECHNICAL REPORT
No. 24 (Mar. 2019)

A Gaussian Filter for Plate Flatness Evaluation System with 3-D Scanner

AOE Shinichiro[*1] MIYAKE Masaru[*2] KABEYA Kazuhisa[*3]

Abstract:

LIDAR (light detection and ranging) system was applied to a plate flatness evaluation system. Plate flatness surfaces are reconstructed from many points generated by LIDAR with a smoothing spline method. We defined a smoothing spline functional with sampling measure weights. The equivalent number of parameters defined on this functional does not depend on the distributions of samples. The approximation of the equivalent number of parameters is derived when the number of samples becomes infinity. This approximation greatly reduced the calculation time needed to estimate the optimal smoothing. The smoothing spline calculation cost was so high that new algorithms (FMM: fast multi-pole method) were introduced and we developed the smoothing engine, which was applied to practical problems. The engine generated clear surfaces and was robust to various dirty points cloud.

1. Introduction

Recently, the 3-D laser scanner (3-D scanner) has become a general-purpose, low-cost technology, and 3-D scanners are now generally applied in various fields. In shipyards, 3-D scanners are used to measure the flatness of steel plates. In the steel industry, 3-D scanners cannot be used for online measurement of the flatness of moving plates in a manner similar to an online shape meter, but they have high portability and are considered to be suitable for online measurement of the flatness of fixed plates.

The problem for application of 3-D scanners to online plate flatness measurement is the difficulty of data handling with the millions of point data measured by a 3-D scanner. These point data, which are projected on the plate surface, are not grid based and are distributed inhomogeneously. Therefore, the procedures for approximation to a curved surface are very complicated. Also, each point datum has measurement error, so a smoothing procedure is necessary to enhance measurement accuracy. Therefore, we applied a smoothing spline method to this problem.

The smoothing spline method is a well-known regression method which is used to estimate non-parametric curves or non-parametric surfaces from noisy samples. This method is a Gaussian filter and is applied to various fields of science and engineering, such as signal processing applications for noise filters[1, 2], image processing applications for image reconstruction[3] and noise filters[4], inverse problems for gravitational and magnetic fields[5], statistical processing applications for medical data[6] and surface reconstructions from noisy data[7, 8] measured by LIDAR (light detection and ranging).

The smoothing parameter in the smoothing spline method enables calculation of a regression function with arbitrary smoothness. When the smoothing parameter is too small, the regression function is overfitted and the function takes a zigzag shape. Conversely, when the smoothing parameter is too large, the regression function becomes too smooth. In this case, the regression function loses important information. Thus, there is an optimal smoothing parameter that makes it possible to calculate an adequate regression function

† Originally published in *JFE GIHO* No. 42 (Aug. 2018), p. 51–56

[*1] Dr. Eng.,
Senior Researcher Deputy General Manager,
Rolling and Processing Research Dept.,
Steel Res. Lab.,
JFE Steel

[*2] Dr. Eng.,
General Manager,
Rolling and Processing Research Dept.,
Steel Res. Lab.,
JFE Steel

[*3] Dr. Eng.,
Executive Assistant,
General Manager,
Res. Planning and Administration Dept.,
Steel Res. Lab.,
JFE Steel

with a better balance between fitness and complexity. The GCV (Generalized Cross Validation) method[9, 10] is often used for automatic estimation of the optimal smoothing parameter. GCV includes iterative calculations of an inverse matrix of a full matrix. However, much time is required to calculate the iterations, and when the number of points is large, it is practically impossible to calculate the optimal smoothing parameter.

Similarly, much time is required to calculate the smoothing spline surface, and when the number of samples is large, it is practically impossible to calculate the smoothing spline surface. Fast methods to calculate a theoretical smoothing spline surface by using FMM (Fast Multi-pole Method) and fast methods to calculate an approximate smoothing spline surface by using a discrete model have been studied. Beatson et al.[11] proposed a fast evaluation method for spline surfaces by using FMM. This method enables a drastic reduction in calculation time. Beatson et al.[12] proposed a fast method based on preconditioned GMRES (Generalized Minimal Residual) iteration to calculate spline coefficients.

In this paper, we introduced original improvements in the conventional smoothing spline method. We define a smoothing spline functional with sampling measure weights[13, 14]. The functional greatly reduces the calculation time needed to estimate the optimal smoothing parameter. We applied our proposed method to practical problems of plate surface estimation for points measured by LIDAR. The fact that our proposed method is appropriate for plate surface reconstructions was clarified[15].

2. Smoothing Thin Plate Spline Regression with Sampling Measure Weights

The smoothing thin plate spline (TPS) functional with weights is defined as

$$\Pi = \sum_{i=1}^{m} \frac{1}{2} \omega_M^{(i)} \left(z_M^{(i)} - f\left(x_M^{(i)}, y_M^{(i)} \right) \right)^2 + \gamma \int_\Omega \frac{1}{2} \left(\nabla^2 f \right)^2 d\Omega \quad \dots (1)$$

where,

$$\nabla = \begin{bmatrix} \dfrac{\partial}{\partial x} & \dfrac{\partial}{\partial y} \end{bmatrix},$$

m is the number of samples, Ω is the area of the sampling region, $\left(x_M^{(i)}, y_M^{(i)} \right)$ (i=1, …, m) is the position of the i th sample, $z_M^{(i)}$ (i=1, …, m) is the value of the i th sample, f is the regression surface, γ is the smoothing parameter, and $\omega_M^{(i)}$ (i=1, …, m) is the weight of the i th sample. We consider the weights are to be defined as

$$\int_0^\Omega g(x,y) d\Omega \simeq \sum_{i=1}^{m} \omega_M^{(i)} g\left(x_M^{(i)}, y_M^{(i)} \right) \quad \dots\dots\dots\dots\dots\dots\dots (2)$$

$$\sum_{i=1}^{m} \omega_M^{(i)} = \Omega, \quad \omega_M^{(i)} \geq 0 \quad (i = 1, \cdots, m)$$

where $g(x,y)$ is an arbitrary function. Eq. (2) is the numerical integral formula. For example, the weights are obtained by the numerical cubature method[16, 17]. In general, however, the weights calculated by numerical cubature are not all positive. If some negative weights are found, the sampling points corresponding to these negative weights must be removed.

Applying the variational principle to the functional of Eq. (1),

$$\begin{aligned} \delta\Pi = \int_\Omega \Big\{ & \gamma \nabla^4 f \\ & + \sum_{i=1}^{m} \omega_M^{(i)} \left(f\left(x_M^{(i)}, y_M^{(i)} \right) - z_M^{(i)} \right) \mathrm{Dirac}\left(x - x_M^{(i)}, y - y_M^{(i)} \right) \Big\} \delta f d\Omega \\ & - \gamma \int_\Gamma \left(\nabla\left(\nabla^2 f \right) \cdot \mu \right) \delta f d\Gamma + \gamma \int_\Gamma \nabla^2 f \left(\delta(\nabla f) \cdot \mu \right) d\Gamma = 0 \quad \dots (3) \end{aligned}$$

where, $\mathrm{Dirac}(x,y)$ is Dirac's delta function, Γ is the boundary of the region Ω, and μ is the normal unit vector of the boundary Γ. From Eq. (3), the partial differential equation of the smoothing TPS is given by

$$\gamma \nabla^4 f + \sum_{i=1}^{m} \omega_M^{(i)} \left(f\left(x_M^{(i)}, y_M^{(i)} \right) - z_M^{(i)} \right) \mathrm{Dirac}\left(x - x_M^{(i)}, y - y_M^{(i)} \right) = 0 \quad \dots\dots (4)$$

and the boundary conditions are given by

$$\nabla^2 f = \nabla\left(\nabla^2 f \right) \cdot \mu = 0 \quad \text{on} \quad \Gamma.$$

In general, a closed-form solution of the partial differential equation (4) is not possible, but if the region Ω is infinity, the solution of the partial differential equation (4) becomes very simple and the regression surface is given by

$$f(x,y) = c_1 + c_2 x + c_3 y + \sum_{i=1}^{m} \frac{d_M^{(i)}}{8\pi} r_M^{(i)}(x,y)^2 \log\left(r_M^{(i)}(x,y) \right) \quad \dots (5)$$

and the constraints are given by

$$\sum_{i=1}^{m} d_M^{(i)} = \sum_{i=1}^{m} x_M^{(i)} d_M^{(i)} = \sum_{i=1}^{m} y_M^{(i)} d_M^{(i)} = 0 \quad \dots\dots\dots\dots\dots\dots\dots (6)$$

where, c_1, c_2, c_3, and $d_M^{(i)}$(i=1, …, m) are the unknown parameters, and $r_M^{(i)}(x,y)$ is defined as

$$r_M^{(i)}(x,y) = \sqrt{\left(x - x_M^{(i)} \right)^2 + \left(y - y_M^{(i)} \right)^2} \quad (i = 1, \cdots, m).$$

Substituting Eq. (5) into Eq. (4),

$$f\left(x_M^{(i)}, y_M^{(i)}\right) + \frac{\gamma}{\omega_M^{(i)}} d_M^{(i)} = z_M^{(i)} \quad (i = 1, \cdots, m) \quad \text{.............. (7)}$$

Eqs. (7) and (6) engender the linear equation system

$$\begin{bmatrix} [A_M] + \gamma[\Omega_M]^{-1} & [P_M] \\ {}^T[P_M] & [O_{3\times3}] \end{bmatrix} \begin{Bmatrix} \{d_M\} \\ \{c\} \end{Bmatrix} = \begin{Bmatrix} \{z_M\} \\ \{O_3\} \end{Bmatrix} \quad \text{......... (8)}$$

where, $[O_{3\times3}]$ is the 3-by-3 zero matrix, $\{O_3\}$ is the 3-by-1 zero vector,

$$[\Omega_M] = \begin{bmatrix} \omega_M^{(1)} & & 0 \\ & \ddots & \\ 0 & & \omega_M^{(m)} \end{bmatrix},$$

$${}^T[A_M] = \left[{}^T\left[a_M\left(x_M^{(1)}, y_M^{(1)}\right)\right] \quad \cdots \quad {}^T\left[a_M\left(x_M^{(m)}, y_M^{(m)}\right)\right] \right],$$

$$[a_M(x,y)] = \frac{1}{8\pi} \times \left[r_M^{(1)}(x,y)^2 \log\left(r_M^{(1)}(x,y)\right) \cdots r_M^{(m)}(x,y)^2 \log\left(r_M^{(m)}(x,y)\right) \right],$$

$$\text{... (9)}$$

$${}^T[P_M] = \left[{}^T\left[p\left(x_M^{(1)}, y_M^{(1)}\right)\right] \quad \cdots \quad {}^T\left[p\left(x_M^{(m)}, y_M^{(m)}\right)\right] \right],$$

$$[p(x,y)] = [1 \quad x \quad y], \quad \text{............................ (10)}$$

$${}^T\{d_M\} = \left[d_M^{(1)} \quad \cdots \quad d_M^{(m)}\right], \quad \text{.......................... (11)}$$

$${}^T\{c\} = [c_1 \quad c_2 \quad c_3], \quad \text{................................ (12)}$$

and

$${}^T\{z_M\} = \left[z_M^{(1)} \quad \cdots \quad z_M^{(m)}\right].$$

The unknown parameters $\{c\}$ and $\{d_M\}$ can be obtained by solving Eq. (8). A regression surface in matrix form

$$f(x,y) = [a_M(x,y)]\{d_M\} + [p(x,y)]\{c\} \quad \text{........... (13)}$$

may be obtained by substituting Eqs. (9), (10), (11) and (12) into Eq. (5). The regression surface can then be obtained by substituting the unknown parameters into Eq. (13).

3. Generalized Cross Validation and Information Criterion

GCV, which is an approximation of leave-one-out cross validation, is one of the most popular methods to obtain the required optimal smoothing parameter. GCV is defined such that the optimal smoothing parameter is the one which minimizes the evaluation function

$$V(\gamma) = \sum_{i=1}^{m} \omega_M^{(i)} \left(z_M^{(i)} - f\left(x_M^{(i)}, y_M^{(i)}\right) \right)^2 \Bigg/ \left(1 - \frac{1}{m} \mathrm{trace}([H]) \right)^2$$

$$\text{... (14)}$$

where $[H]$ is the so-called Hat matrix, defined as

$$\{f_M\} = [H]\{z_M\} \quad \text{.................................. (15)}$$

where

$${}^T\{f_M\} = \left[f\left(x_M^{(1)}, y_M^{(1)}\right) \quad \cdots \quad f\left(x_M^{(m)}, y_M^{(m)}\right) \right].$$

Substituting into Eq. (15) the regression surface of Eq. (13), in which the unknown parameters $\{c\}$ and $\{d_M\}$ from Eq. (8) are substituted, the Hat matrix of the smoothing TPS with weights can be written as

$$[H] = \left[[A_M] \quad [P_M] \right] \begin{bmatrix} [A_M] + \gamma[\Omega_M]^{-1} & [P_M] \\ {}^T[P_M] & [O_{3\times3}] \end{bmatrix}^{-1} \begin{bmatrix} [I_{m\times m}] \\ [O_{3\times m}] \end{bmatrix}$$

$$\text{... (16)}$$

where, $[I_{m\times m}]$ is the m-by-m identity matrix, and $[O_{3\times m}]$ is the 3-by-m zero matrix.

It is known that the GCV evaluation function of Eq. (14) is associated with the information criterion. In particular, AIC[18] is given by

$$AIC = -2LL + 2k \quad \text{.................................. (17)}$$

where, LL is the maximum log likelihood defined as

$$LL = -\frac{m}{2} \log\left(\sum_{i=1}^{m} \omega_M^{(i)} \left(z_M^{(i)} - f\left(x_M^{(i)}, y_M^{(i)}\right) \right)^2 \right),$$

and k is the number of parameters or the degree of freedom for a regression model. AIC is one of the most popular and simplest information criteria; it is nearly equivalent to the GCV evaluation function when m is large. Eq. (14) can be transformed to the information criterion

$$IC_{GCV} = m \log(V(\gamma)) = -2LL - 2m \log\left(1 - \frac{\mathrm{trace}([H])}{m} \right)$$

$$\text{.. (18)}$$

by using the increasing function. In the limit of infinite samples, Eq. (18) becomes

$$AIC = -2LL + 2\,\mathrm{trace}\left(\left[H\right]\right). \quad (19)$$

Comparing Eq. (17) with Eq. (19), $\mathrm{trace}\left(\left[H\right]\right)$ replaces the number of parameters for the smoothing TPS. Consequently, ENOP (Equivalent Number of Parameters) is defined as

$$k_{GCV} = \mathrm{trace}\left(\left[H\right]\right). \quad (20)$$

As the number of samples becomes large, the time required to calculate ENOP becomes prohibitively long, because ENOP includes computing the m+3 -by-m+3 inverse matrix. Moreover, the inverse matrix must be computed every time the smoothing parameter is changed.

4. Approximation of Equivalent Number of Parameters

In the limit of infinite samples, the partial differential equation of the smoothing TPS with sampling measure weights, Eq. (4), becomes

$$\gamma\nabla^4 f + f - z_M = 0 \quad (21)$$

where z_M is the sampling value function. Applying the Laplace transformation to Eq. (21),

$$f\left(s_1, s_2\right) = h\left(s_1, s_2\right) z_M\left(s_1, s_2\right) \quad (22)$$

where, s_1 and s_2 are the Laplace variables in the x -axis and the y -axis, and $h\left(s_1, s_2\right)$ is the transfer function given by

$$h\left(s_1, s_2\right) = \left\{\gamma\left(s_1^{\,2} + s_2^{\,2}\right)^2 + 1\right\}^{-1}. \quad (23)$$

Comparing Eq. (22) and Eq. (15), it can be understood that the transfer function $h\left(s_1, s_2\right)$ plays the same role as the Hat matrix. Applying the Fourier transformation to Eq. (23), the frequency response function $h\left(\omega_1, \omega_2\right)$ is given by

$$\begin{aligned} h\left(\omega_1, \omega_2\right) &= \left\{\gamma\left(\left(j\omega_1\right)^2 + \left(j\omega_2\right)^2\right)^2 + 1\right\}^{-1} \\ &= \left\{\gamma\left(\omega_1^{\,2} + \omega_2^{\,2}\right)^2 + 1\right\}^{-1} \end{aligned} \quad (24)$$

where, j is an imaginary unit, and ω_1 and ω_2 are the angular frequencies in the x -axis and the y -axis. The frequency response function $h\left(\omega_1, \omega_2\right)$ shows that the smoothing TPS acts as a low pass filter and a Gaussian filter with phase compensation.

When the region Ω is rectangular ($L_1 \times L_2$), the degree of freedom k_1 for trigonometric functions in the x -axis is defined as

$$k_1 = L_1 / L_{\omega_1} \quad (25)$$

where L_{ω_1} is the half wavelength given by

$$L_{\omega_1} = \pi / \omega_1 . \quad (26)$$

Substituting Eq. (26) into Eq. (25),

$$k_1 = L_1 \omega_1 / \pi . \quad (27)$$

Applying the above formulation to the y -axis, the degree of freedom k_2 in the y -axis is given by

$$k_2 = L_2 \omega_2 / \pi . \quad (28)$$

Substituting Eqs. (27) and (28) into Eq. (24), the response function $h\left(k_1, k_2\right)$ for the degrees of freedom k_1 and k_2 has the form

$$h\left(k_1, k_2\right) = \left\{\gamma\left(\left(\frac{\pi}{L_1}k_1\right)^2 + \left(\frac{\pi}{L_2}k_2\right)^2\right)^2 + 1\right\}^{-1},$$

From the definition of ENOP, Eq. (20), ENOP is the summation of eigenvalues of the Hat matrix; then, ENOP for an infinite number of samples is given by

$$\begin{aligned} k_A\left(\gamma\right) &= \int_0^\infty \int_0^\infty h\left(k_1, k_2\right) dk_1 dk_2 \\ &= \int_0^\infty \int_0^\infty \left\{\gamma\left(\left(\frac{\pi}{L_1}k_1\right)^2 + \left(\frac{\pi}{L_2}k_2\right)^2\right)^2 + 1\right\}^{-1} dk_1 dk_2 . \end{aligned} \quad (29)$$

Thus, k_A becomes the approximation of ENOP. Applying the changes of the variables

$$r = \left(\frac{\pi}{L_1}k_1\right)^2 + \left(\frac{\pi}{L_2}k_2\right)^2, \quad \tan\theta = \frac{L_1 k_2}{L_2 k_1}$$

to the integral of Eq. (29), the approximation of ENOP, k_A, becomes

$$\begin{aligned} k_A\left(\gamma\right) &= \frac{L_1 L_2}{2\pi^2} \int_0^{\frac{\pi}{2}} d\theta \int_0^\infty \frac{1}{\gamma r^2 + 1} dr \\ &= \frac{L_1 L_2}{8\pi} \mathrm{B}\left(\frac{1}{2}, \frac{1}{2}\right) \gamma^{-\frac{1}{2}} = \frac{L_1 L_2}{8} \gamma^{-\frac{1}{2}} \end{aligned} \quad (30)$$

where B is Euler's Beta function. This approximation of ENOP, k_A, is a very simple expression and does not

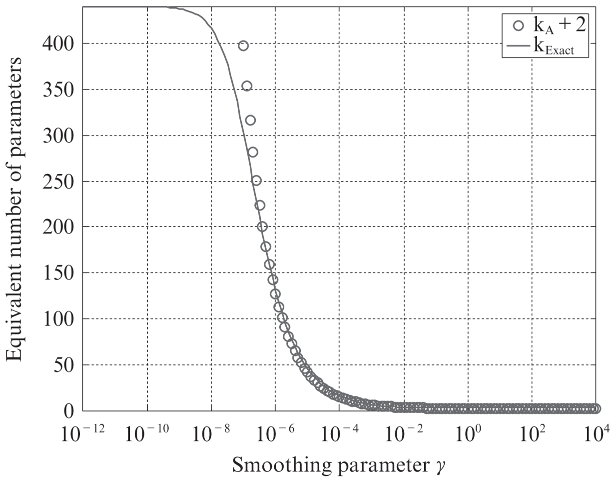

Fig. 1 Equivalent number of parameters

depend on the distributions of samples. The approximation of ENOP, Eq. (30), is only applied to a rectangular region. The approximation of ENOP generalized for application to an arbitrary region is given by

$$k_A(\gamma) = \frac{\Omega}{8}\gamma^{-\frac{1}{2}}. \quad (31)$$

The above-mentioned derivation of the approximation of ENOP (31) is formal. The formulation for the smoothing spline curve can be found in Craven et al.[9] and Golub et al.[10]. The details of the theories are described in these references.

Figure 1 shows the approximation of ENOP obtained from Eq. (31) and the exact ENOP, k_{GCV}, obtained from Eq. (20) when the smoothing TPS is used, the number of samples is 21* 21=441, and the sampling region is [0,1]×[0,1]. Bias is added to the approximation of ENOP to enable comparison with the exact ENOP. The approximation of ENOP, k_A, shows good agreement with the exact ENOP, k_{GCV}, in the ENOP range from 0 to half the number of samples; however, the correlation is not good for ENOP ranging from half to the total number of samples. The typical practice is that ENOP should not be used when it is larger than half the number of samples. Therefore, if the optimal ENOP decided by GCV or information criteria is more than half the number of samples, the number of samples should be increased.

5. Plate Surface Estimation by Using LIDAR and Smoothing TPS with Sampling Measure Weights

Figure 2 shows the point cloud of samples measured with a LIDAR on a plate surface. The plate length is 5.475 m and the plate width is 2.143 m. The x -axis is the rolling direction, and the values of the x -axis are ten times the actual ones. The y -axis is the plate width direction. The distance in the longitudinal direction x is decoupled because the wavelength in the longitudinal direction x is shorter than that in the width direction y and to show both wavelengths in the same dimension. The distribution of samples is not homogeneous. The number of samples is 25 691. The values of the samples include measurement error of 2 mm. This error value is taken from the specification of the 3-D laser scanner, which is a Photon 120 manufactured by FARO Corp. The samples (**Fig. 2**) are interpolated into a DEM (digital elevation model) in **Fig. 3** with a mesh of triangles. Although the DEM of the plate surface has a zigzag shape, the actual plate surface was not zigzagged, as it was a rolled plate. The zigzag shape derives from LIDAR measurement error. The zigzag shape is considered to be eliminated by the smoothing TPS with sampling measure weights.

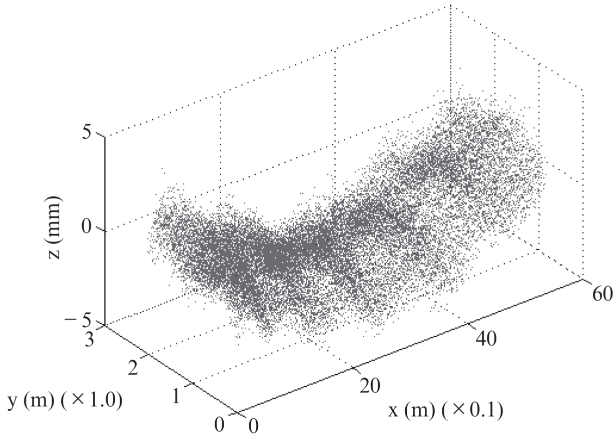

Fig. 2 Plate surface point cloud

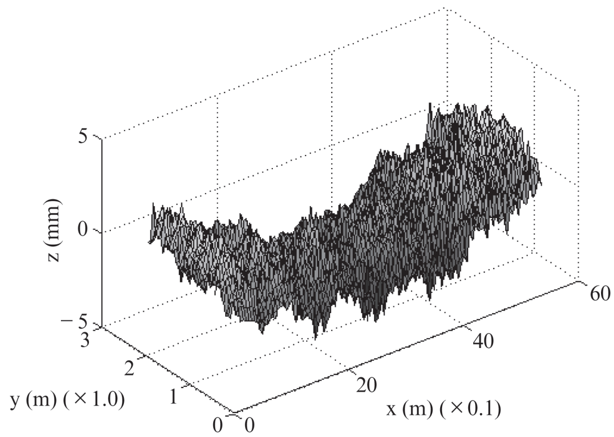

Fig. 3 Plate surface DEM

As the number of samples becomes larger (experimentally more than 3 000), the time required to solve the system of Eq. (8) becomes prohibitively long. In this case, in order to evaluate the value of Eq. (13), we applied a fast calculation method based on FMM (Fast Multipole Method) proposed by Beatson et al.[11] and solved the system of Eq. (8) with GMRES (Generalized

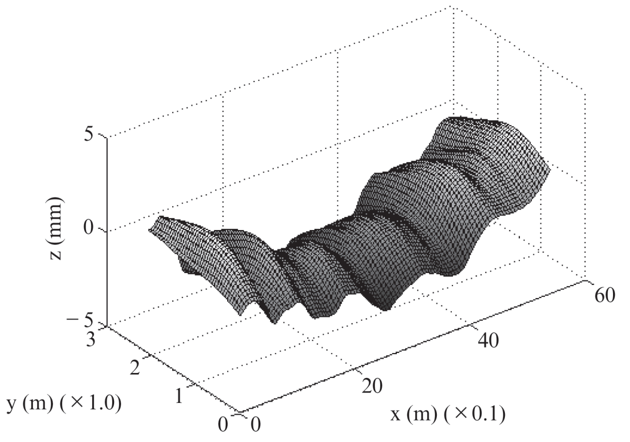

Fig. 4 Result of optimal regression for plate surface

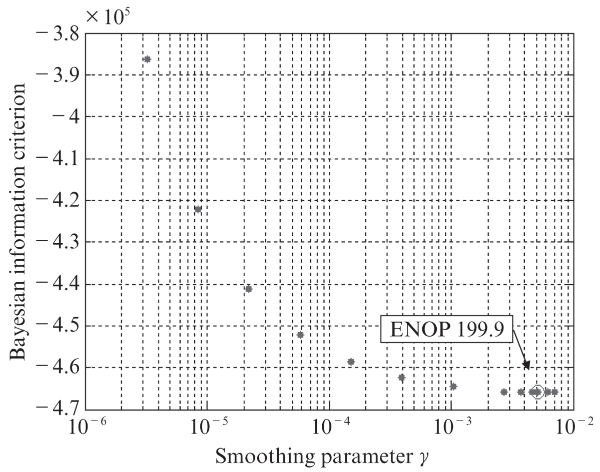

Fig. 5 Results of Bayesian information criterion

Minimal Residual Method). In the preconditioning of GMRES, the approximated cardinal functions proposed by Beatson et al.[12] were used as reference.

In this case, we use BIC (Bayesian information criterion) defined as

$$BIC_A = m\log\left(\sum_{i=1}^{m}\omega_M^{(i)}\left(z_M^{(i)} - f\left(x_M^{(i)}, y_M^{(i)}\right)\right)^2\right)$$
$$-\log m \times m\log\left(\left(1-\frac{k_A}{m}\right)^2\right)$$

to decide the optimal smoothing parameter. Practically speaking, application of the GVC method is not possible with large-scale samples. **Figure 5** shows the search result of the optimal smoothing parameter. The horizontal axis shows the smoothing parameter. The vertical axis shows BIC. The points show the search process, and the circle at the lower right shows the optimal search result. The value of the optimal smoothing parameter is 5.09×10^{-3}, and the value of ENOP is 199.9. **Figure 4** shows the estimated plate surface for the optimal smoothing parameter. Good agreement between the plate surface shown in Fig. 4 and the result of manual measurement was confirmed.

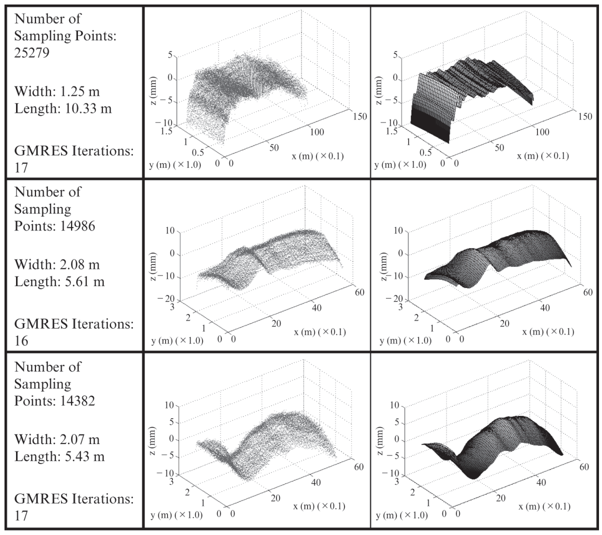

Fig. 6 Results of regressions for plate surfaces

The plate surface was estimated on a 2.66 GHz Intel(R) Core(TM)2 Quad CPU with a 3.25 GB RAM and a Microsoft Visual C++ 2005 on a Windows XP x86. It took 9.8 s to calculate the plate surface in Fig. 4 and 226 s to calculate the optimal smoothing parameter.

The distribution of the wavelength on a plate surface does not depend on the size of plates if the plates are produced under the same processing conditions. Let the representative half wavelength on a plate surface be L_ω. From Eqs. (25) and (31), the smoothing parameter for the smoothing TPS is given by

$$\gamma = L_\omega{}^4/64\ . \quad (32)$$

The smoothing parameter depends on only the half wavelength, L_ω. Eq. (32) means that it is not necessary to calculate the optimal smoothing parameter whenever the plate to be measured changes. **Figure 6** shows the surface regressions when the same smoothing parameter is used.

6. Conclusions

In this paper, we proposed a method for reconstructing the surface shape of steel plates from a large number of point data obtained by a 3-D scanner. The following conclusions were drawn from the theoretical, numerical, and experimental investigations carried out in this work:

(1) A smoothing TPS method with sampling measure weights was defined theoretically.
(2) In the limit of infinite samples, the transfer function and the frequency response function for the

smoothing TPS system with sampling measure weights were solved theoretically.

(3) The approximation of ENOP was derived theoretically from the frequency response function. We confirmed that the approximation agreed with the theoretical ENOP.

(4) The information criteria including the approximation of ENOP enabled calculation of the optimal smoothing parameter.

(5) We applied the proposed method to the problem of actual large-scale samples measured by LIDAR. The results clarified the fact that engineering applications of the method are possible.

REFERENCES

1) De Nicolao, G.; Ferrari-Trecate, G. IEEE T. Neural Networ. 2001, vol. 12, p. 228.
2) Unser, M.; Blu, T. IEEE T. Signal Proces. 2005, vol. 53, p. 2146.
3) Gumerov, N.A.; Duraiswami, R. SIAM J. Sci. Comput. 2007, vol. 29, p. 1876
4) Gotchev, A.; Egiazarian, K. ISPA 2001, Proc. 2nd Int. Symp. on Image and Signal Processing and Analysis, IEEE, Piscataway, NJ, 2001.
5) Haber, E.; Oldenburg, D. Computat. Geosci. 2000, vol. 4, p. 41.
6) Lin, X.; Wahba, G.; Xiang, D.; Gao, F.; Klein, R.; Klein, B. Ann. Stat. 2000, vol. 28, p. 1570.
7) Carr, J.C.; Beatson, R.K.; Cherrie, J. B.; Mitchell, T.J.; Fright, W.R.; McCallum, B.C.; Evans, T.R. Proc. 28th Annu. Conf. Computer Graphics and Interactive Technique. ACM, New York, 2001, p. 67.
8) Gumerov, N.A.; Duraiswami, R. J. Comput. Phys. 2006, vol. 215, p. 363.
9) Craven, P.; Wahba, G. Numer. Math. 1979, vol. 31, p. 377.
10) Golub, G.H.; Heath, M.; Wahba, G. Technometrics. 1979, vol. 21, p. 215.
11) Beatson, R.K.; Newsa, G.N. Comput. Math. Appl. 1992, vol. 2, p. 7.
12) Beatson, R.K.; Cherrie, J.B.; Mouat, C.T. Adv. Comput. Math. 1999, vol. 11, p. 253.
13) Aoe, S.; Hulbert, G.M. 9th US National Cong. on Computational Mechanics, USACM, San Francisco, 2007.
14) JFE Steel. Aoe, S.; Uetake, N.; Hayashi, H. Japanese Patent Publication No. 2012–37313. 2012.
15) Aoe, S.; Miyake, M.; Kabeya, K. ISIJ International. 2017, vol. 57, p. 1054.
16) JFE Steel. Aoe. S. Japanese Patent Publication No. 2002–365047. 2002.
17) Sommariva, A.; Vianello, M. Computing. 2006, vol. 76, p. 295.
18) Akaike, H. IEEE T. Automat. Contr. 1974, vol. 19, p. 716.